Control System Design for an Electrostatic Strain Wave Motor

Design Proposal

Team DoSWM

Joseph Serra
934-512-465

ENGR 416 Interdisciplinary Capstone
Oregon State University

January 16, 2026

1 Background and Context

Electrostatic actuators operate on fundamentally different principles than magnetic motors. While magnetic motors generate force through the interaction of magnetic fields with current-carrying conductors, electrostatic actuators produce force directly from electric field attraction between charged surfaces. The force density scales with the square of the electric field strength and the dielectric constant of the insulating material. This relationship, expressed as $F = \frac{1}{2}\epsilon_0\epsilon_r E^2$, where ϵ_0 represents the permittivity of free space, ϵ_r the relative permittivity, and E the electric field strength, reveals both the promise and challenge of electrostatic actuation [1, 2].

Traditional electrostatic motors required 5,000–10,000 V to generate useful force because common dielectric materials have relative permittivity around 3–4. At these voltages, power electronics become prohibitively expensive, requiring specialized high-voltage transistors, isolation transformers, and extensive safety measures. Commercial gate drivers rarely exceed 1,200 V ratings, and even specialized high-voltage operational amplifiers typically operate below 200 V. This creates a significant gap between what electrostatic motors traditionally required and what practical electronics could deliver.

The breakthrough enabling this project came from Gravert et al., who demonstrated P(VDF-TrFE-CTFE) terpolymer as a dielectric material with relative permittivity around 40 [1]. This order-of-magnitude improvement in dielectric constant translates directly to voltage reduction while maintaining equivalent force. Their untethered robotic fish, powered by a compact lithium-polymer battery at 900–1,100 V, proved that electrostatic actuation could operate within the range of available power semiconductors.

However, transitioning from simple antagonistic actuation in a swimming robot to continuous rotation in a motor introduces significant control challenges. The ferroelectric nature of the high-permittivity dielectric creates hysteresis and charge retention effects absent in conventional capacitors [1]. Unlike ideal dielectrics that immediately discharge when voltage is removed, ferroelectric materials retain polarization that must be actively managed through bipolar driving schemes. Additionally, the dielectric properties vary with frequency, temperature, and applied field strength, requiring adaptive control strategies.

The strain wave gear topology selected for this project further complicates control requirements. The approach replaces the mechanical cam of traditional strain wave drives with distributed electrostatic actuators that must be precisely coordinated to synthesize the traveling wave electronically. This requires phase synchronization accuracy better than $\pm 2\%$ to prevent torque ripple and potential stalling, significantly tighter than the $\pm 10\%$ tolerance acceptable in the antagonistic fish actuator.

Previous work by the team lead validated the strain wave concept using magnetic solenoids arranged radially around a 3D-printed flexspline [3]. While successful in demonstrating continuous rotation, the magnetic prototype revealed limitations that motivated the transition to electrostatic actuation: resistive heating in coils limited duty cycle, moving permanent magnet cores added mechanical complexity, and rigid magnetic components created stress concentrations in the flexspline. These findings informed the requirements for the electrostatic control system, particularly the need for high efficiency to enable continuous operation and flexible control of force profiles to accommodate mechanical compliance.

2 Project Scope Summary

This capstone project develops a complete electrostatic strain wave motor system as a demonstrator for next-generation robotic actuation. The motor addresses fundamental limitations of magnetic motors in robotics applications: excessive weight from copper windings and rare-earth magnets, dangerous kinetic energy storage in high-speed gearboxes, and significant heat generation requiring cooling systems. The interdisciplinary team consists of four students: Ben Cantarero and Josh Elliot in mechanical engineering, and Alexander Roller and Joseph Serra from electrical and computer engineering.

The project leverages recent breakthroughs in ferroelectric materials, specifically hydraulically amplified low-voltage electrostatic (HALVE) actuators that reduce operating voltage from 5,000–10,000 V to approximately 1,000 V [1]. This builds on earlier HASEL actuator research [2, 4] but uses high-permittivity ferroelectric dielectrics to achieve the voltage reduction. The motor combines six HALVE actuators arranged radially around a strain wave gear, creating continuous rotation through coordinated three-phase excitation.

The electrical engineering work is divided between two team members. Alexander Roller is responsible for the high-voltage control board, including H-bridge circuits to control actuator polarity and managing the unique challenges of ferroelectric materials including charge retention and frequency-dependent dielectric properties. The author's primary responsibility involves developing the power electronics subsystem and control interface: the smart power supply with USB-C Power Delivery input (5–12 V), lithium-polymer battery management, buck conversion to 5 V, DC-DC boost conversion to 1,000 V, the ESP32-C6 firmware for three-phase PWM signal generation, and the web-based graphical user interface for motor control. Together, these subsystems must coordinate precise timing across six actuators while maintaining electrical isolation between phases at kilovolt potentials.

3 Design Process

The control system design required solving several interconnected challenges: generating three-phase high-voltage waveforms from a 12 V battery, maintaining phase isolation at kilovolt potentials, and managing ferroelectric material characteristics. The system was decomposed into five subsystems: power conversion, signal generation, isolation, switching circuits, and feedback control. Each subsystem had multiple implementation options evaluated through analysis, simulation, and limited testing.

For initial concept validation, SPICE simulation was used to model different circuit topologies.

The high-voltage nature of the system made physical prototyping dangerous and expensive, so extensive simulation preceded any hardware implementation. KiCad served as the primary tool for schematic capture and printed circuit board (PCB) layout once the design converged. The decision to use KiCad over alternatives like Altium or Eagle was driven by its open-source nature, allowing all team members to access the design files without licensing constraints.

Component selection involved extensive research into high-voltage semiconductors. Power MOSFETs rated above 1,000 V are typically designed for industrial applications, priced at $50–100 per device. Gate drivers at these voltages require careful attention to isolation ratings and dead-time generation to prevent shoot-through.

Component placement on the PCB required careful attention to high-voltage design rules. Traces carrying 1,000 V maintain 3 mm clearance from any grounded conductor, with slots milled in the PCB to extend creepage distances. The high-voltage section uses a separate ground plane isolated from the control electronics except at a single star point, preventing ground loops that could couple switching noise into sensitive analog circuits.

Isolation between the low-voltage control signals and high-voltage switching circuits presents a significant design challenge. At low voltages (under 200 V), operational amplifiers can provide level shifting and signal conditioning with adequate isolation. At kilovolt levels, traditional approaches require pulse transformers to couple gate drive signals across the isolation barrier, adding cost, complexity, and introducing bandwidth limitations from transformer parasitics. Optocouplers provide an elegant alternative: an LED on the low-voltage side optically couples to a phototransistor on the high-voltage side, achieving galvanic isolation without magnetic components. This approach maintains signal fidelity at the switching frequencies required for PWM control while ensuring that any high-voltage fault cannot propagate back to destroy the control electronics. Figure 1 illustrates this isolation topology.

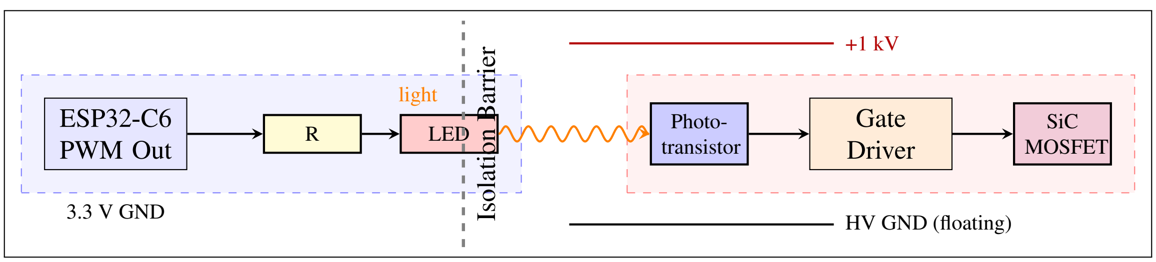

Figure 1: Optocoupler isolation circuit topology. The ESP32-C6 PWM signal drives an LED through a current-limiting resistor. Light couples across the isolation barrier to a phototransistor, which triggers the gate driver. This provides galvanic isolation between the 3.3 V control ground and the floating high-voltage ground, preventing fault propagation.

4 Final Design

The control system architecture consists of three primary boards: a smart power supply, a microcontroller board, and a high-voltage switching board. Figure 2 illustrates the signal and power flow through the complete system.

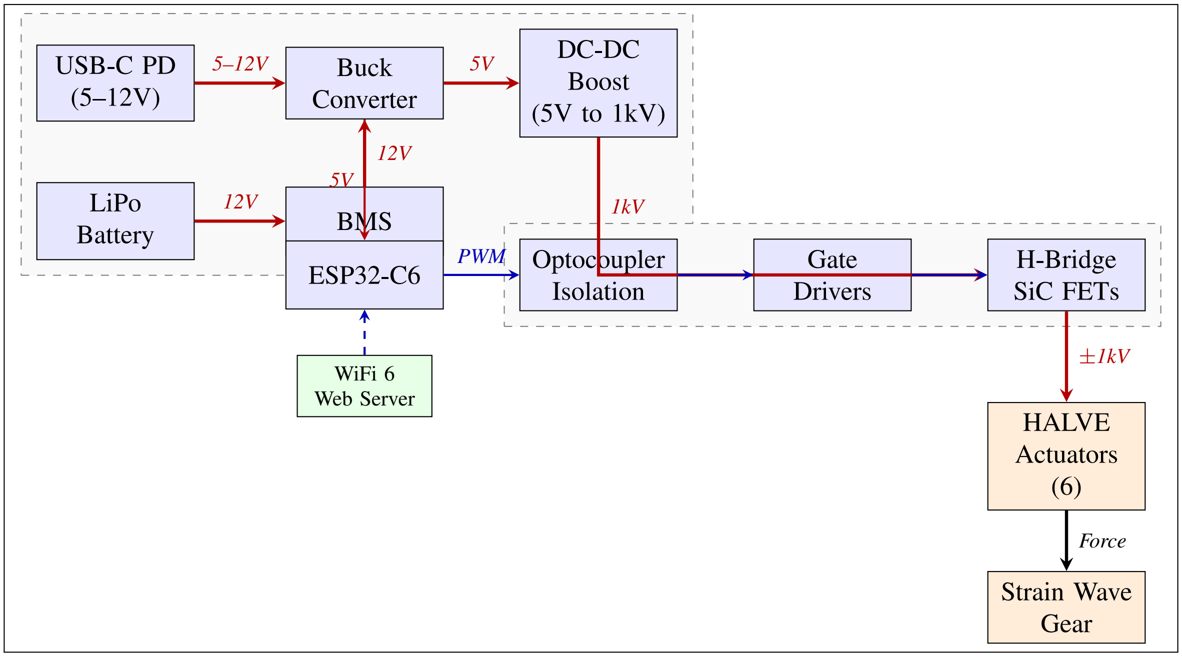

Figure 2: Control system block diagram showing power flow (thick red arrows) and signal flow (thin blue arrows). Either USB-C PD (5–12 V) or the LiPo battery through the BMS (12 V) feeds the buck converter, which outputs 5 V to both the ESP32-C6 and the DC-DC boost converter. The boost converter generates 1 kV for the actuators.

The smart power supply accepts input from either USB-C Power Delivery (5–12 V) or an onboard lithium-polymer battery (12 V) through a BMS. A buck converter steps the input to 5 V, feeding both the ESP32-C6 and the XP Power Q10-5 boost converter [5], which generates 1,000 V for the actuators. The overall power supply architecture draws inspiration from previous compact high-voltage supplies for soft actuators [6].

The ESP32-C6 generates three-phase PWM signals for the six actuators. Users can connect via WiFi or USB to adjust frequency, duty cycle, and phase relationships through a web-based interface.

The high-voltage board contains optocoupler isolation circuits that provide galvanic separation between the low-voltage control signals and the kilovolt switching circuits. Gate drivers amplify the isolated signals to switch the SiC MOSFETs in the H-bridge configuration. The H-bridge topology allows bipolar voltage application to each actuator pair, which is necessary to manage charge retention in the ferroelectric dielectric material.

5 Design Rationale

The selected design emerged as optimal through systematic evaluation against project requirements. The decision to use PWM rather than linear amplification fundamentally shaped the architecture—

linear amplification's efficiency penalty at high voltage makes it impractical. The H-bridge approach achieves efficiency above 95%, enabling battery-powered operation.

The choice of 1,000 V operating voltage balances force generation against component availability. Components rated above 1,200 V enter industrial pricing territory, while lower voltage would require larger or more numerous actuators. The selected voltage provides adequate margin below the 1,200 V rating of available SiC MOSFETs.

The distributed architecture with separate power supply and high-voltage boards improves safety by isolating high voltage to a single enclosable board, accelerates development through parallel work, and enables modularity for testing different configurations or future expansion to six-phase or nine-phase drives.

The decision to implement USB-C Power Delivery rather than a simple barrel jack connector future-proofs the design and simplifies the user interface by handling both charging and data communication through a single port.

Selecting the ESP32-C6 over alternatives like STM32 or Arduino provides critical wireless capabilities for the control architecture. The integrated WiFi enables a web-based control interface hosted directly on the microcontroller, eliminating the need for external computers or proprietary software—users can control the motor from any web browser over WiFi, or connect directly via USB. The custom firmware in C provides deterministic control over timing-critical PWM generation. At under $10, the ESP32-C6 provides exceptional value compared to industrial motor controllers.

The design satisfies key customer requirements: torque density comparable to geared magnetic motors, operation at voltages compatible with commercial semiconductors, inherent safety through elimination of rotational inertia, and cost-effectiveness through commodity components.

6 Project Timeline

Development proceeds in two phases aligned with the academic calendar. During the current fall term, the focus is on completing the control system design, finalizing PCB layouts, and ordering components. Winter term will involve PCB fabrication, firmware development for the ESP32-C6, and physical motor design testing with the goal of demonstrating a functional motor.

Key milestones include: PCB rework complete by Week 3 of winter term, physical motor design testing throughout winter term, and first motor rotation by Week 10. Achieving rotation demonstrates torque production, validating the complete control system as functional.

7 Conclusion

This design proposal presents a comprehensive control system for an electrostatic strain wave motor that addresses fundamental limitations of both magnetic motors and previous electrostatic designs. The systematic design process evaluated multiple architectures, ultimately selecting a PWM-based approach that balances performance, cost, and feasibility within project constraints.

The selected design achieves all critical requirements: operation at 1,000 V using commercially available components, battery-powered portability through efficient power conversion, precise phase control via digital PWM generation, and modular architecture enabling parallel development. The web-based control interface makes the system accessible without specialized software.

Successful completion will validate electrostatic motors as viable alternatives for robotics applications requiring high torque density, inherent safety, and high efficiency.

References

[1] Gravert, S.-D., Varini, E., Kazemipour, A., Michelis, M. Y., Buchner, T., Hinchet, R., and Katzschmann, R. K., “Low-Voltage Electrohydraulic Actuators for Untethered Robotics,” *Science Advances*, Vol. 10, No. 1, 2024. https://doi.org/10.1126/sciadv.adi9319

[2] Acome, E., Mitchell, S. K., Morrissey, T. G., Emmett, M. B., Benjamin, C., King, M., Radakovitz, M., and Keplinger, C., “Hydraulically Amplified Self-Healing Electrostatic Actuators with Muscle-Like Performance,” *Science*, Vol. 359, No. 6371, 2018, pp. 61–65. https://doi.org/10.1126/science.aao6139

[3] Cantarero, B., “Variable Speed Test of 140 mm Magnetic Strain Wave Motor,” Google Drive, 2025. Retrieved October 12, 2025.

[4] Mitchell, S. K., Wang, X., Acome, E., Martin, T., Ly, K., Kellaris, N., Venkata, V. G., and Keplinger, C., “An Easy-to-Implement Toolkit to Create Versatile and High-Performance HASEL Actuators for Untethered Soft Robots,” *Advanced Science*, Vol. 6, No. 14, 2019. https://doi.org/10.1002/advs.201900178

[5] XP Power, “Q Series DC-DC Converters,” XP Power Ltd., Datasheet, 2024. https://www.xppower.com/portals/0/pdfs/SF_Q.pdf

[6] Mitchell, S. K., Martin, T., and Keplinger, C., “A Pocket-Sized Ten-Channel High Voltage Power Supply for Soft Electrostatic Actuators,” *Advanced Materials Technologies*, Vol. 7, No. 2, 2022. https://doi.org/10.1002/admt.202101469

This writeup was prepared with assistance from Claude by Anthropic, a large language model. The AI was used to aid in research, help structure a technical outline, ensure adherence to the MIME Capstone Design Style Guide formatting requirements, and refine language for clarity and conciseness. All technical content, research citations, project scope definitions, and engineering decisions reflect the author’s own work and understanding of the project.